

Optimal Control of Differentially Flat Systems is Surprisingly Easy[★]

Logan E. Beaver^a, Andreas A. Malikopoulos^b

^a*Division of Systems Engineering, Boston University, Boston, MA, USA, 02215*

^b*Department of Mechanical Engineering, University of Delaware, Newark, DE, 19716*

Abstract

As we move to increasingly complex cyber-physical systems (CPS), new approaches are needed to plan efficient state trajectories in real-time. In this paper, we propose an approach to significantly reduce the complexity of solving optimal control problems for a class of CPS with nonlinear dynamics. We exploit the property of differential flatness to simplify the Euler-Lagrange equations that arise during optimization, and this simplification eliminates the numerical instabilities that plague optimal control in general. We also present an explicit differential equation that describes the evolution of the optimal state trajectory, and we extend our results to consider both the unconstrained and constrained cases. Furthermore, we demonstrate the performance of our approach by generating the optimal trajectory for a 2D crane system. We show in simulation that our approach is able to generate the unconstrained optimal trajectory in 1.5 ms and a constrained optimal trajectory in 184 ms.

Key words: Optimal Control; Differential Flatness; Constrained Optimization; Optimization; Nonlinear Control;

1 Introduction

There is an increasing demand to extend the boundaries of autonomy in cyber-physical systems (CPS) using experimental testbeds (see: Rubenstein et al. (2012); Jang et al. (2019); Beaver et al. (2020); Chalaki et al. (2022)) and outdoor experiments (see: Vásárhelyi et al. (2018); Mahbub and Malikopoulos (2020); Chalaki et al. (2022)). As CPS achieve higher autonomy levels, they will be forced into complicated interactions with other agents and the surrounding environment (Malikopoulos et al., 2021; Beaver and Malikopoulos, 2021; Oh et al., 2017). These autonomous agents must be able to react quickly to their environment and re-plan efficient trajectories. To this end, we propose a new method to simplify real-time optimal trajectory planning by exploiting differential flatness.

A system is differentially flat if there exist a set of endogenous *flat* variables, also called *outputs*, such that the original state and control variables can be written as an explicit function of the flat variables and a finite number

of their derivatives. This yields an equivalent flat system that is completely described by integrator dynamics. It is significantly easier to generate control trajectories in the flat space, wherein the trajectories can be exactly mapped back to the original coordinate system. Differentially flat systems have garnered significant interest since their introduction by Fliess et al. (1995), and it has been shown that generating trajectories in the flat space can reduce computational time by at least an order of magnitude (e.g., see: Petit et al. (2001)). Differentially flat systems are closely related to feedback linearizable systems (Lévine, 2007); however, the standard control techniques for flat systems are distinct from feedback linearization.

The overwhelming majority of research on trajectory generation with differential flatness uses collocation techniques, i.e., finding optimal parameters for a set of basis functions in the flat space. Under this approach, a designer selects an appropriate basis function for their application, e.g., polynomial splines in Mellinger and Kumar (2011); Sreenath et al. (2013), Bezier curves in Milam (2003), Fourier transforms in Ogunbodede (2020), or piece-wise constant functions in Kolar et al. (2017). The parameters of these basis functions are optimally determined to yield the optimal trajectory for the selected basis. A rigorous overview of this approach

[★] This research was supported by NSF under Grants CNS-2149520 and CMMI-2219761.

Email addresses: lebeaver@bu.edu (Logan E. Beaver), andreas@udel.edu (Andreas A. Malikopoulos).

is given in the recent textbook by [Sira-Ramirez and Agrawal \(2018\)](#).

In contrast, we propose an indirect approach that seeks a solution by solving a set of optimality conditions. A recently proposed technique to solve a limited class of optimal control problems is the Method of Evolving Junctions (MEJ) (see [Li et al. \(2017\)](#)), which was applied to optimal navigation of flow fields in [Zhai et al. \(2022\)](#). Similar to MEJ, our approach generates a collection of optimal trajectory segments between discrete junctions. However, as our approach exploits the properties of differential flatness, we do not impose the strong limits on the size of the state space or the form of the objective function that MEJ requires. Furthermore, instead of using a stochastic differential equation to generate the junction states, solving the optimization problem in the flat space enables us to solve the problem of determining optimal junctions using a one-dimensional root-finding algorithm.

There are weaker and more general results for the so-called maximal inversion approach by [Chaplais and Petit \(2007, 2008\)](#), which proves that the optimality conditions for a feedback linearizable system can be separated into two parts—one describing the optimal state trajectory, and the other describing the optimal costate trajectory. This separation result is significant, as the general optimality conditions couple the evolution of the states and costates, which can lead to significant numerical instabilities (see: [Bryson \(1996\)](#)). While [Chaplais and Petit \(2008\)](#) proved that the optimality conditions are separable, in this paper, we provide the analytical form of the ordinary differential equation that explicitly describes their evolution. Furthermore, while [Chaplais and Petit \(2008\)](#) considers control-affine nonlinear systems, our proposed approach does not require affinity in the control variables. More recent work following this approach employs saturation functions to handle trajectory constraints, e.g., [Graichen et al. \(2010\)](#), whereas our approach explicitly generates constrained optimal trajectories. Finally, we also derive the optimal boundary conditions in the flat space, which, to the best of our knowledge, has not been addressed in the literature to date. The contributions of this paper are:

- We present a set of ordinary differential equations that describe the evolution of the costates as explicit functions of the state and control variables (Theorem 1).
- We derive optimality conditions that are independent of the costates (Theorem 2). This independence property holds for interior-point (Section 3.2) and trajectory (Section 3.3) constraints.
- We derive equivalent boundary conditions for the state and control variables when an initial or final state is left free or when the final time is unknown (Section 3.4).

The remainder of the article is organized as follows. In

Section 2, we provide the modeling framework and enumerate our assumptions before presenting our main theoretical results in Section 3. Then, in Section 4, we provide an illustrative example of controlling a nonlinear overhead crane with bounds on its position. Finally, we draw concluding remarks and present directions of future work in Section 5.

2 Problem Formulation

Consider the nonlinear dynamical system,

$$\dot{\mathbf{x}}(t) = \mathbf{f}(\mathbf{x}(t), \mathbf{u}(t)), \quad (1)$$

where $\mathbf{x}(t) \in \mathcal{X} \subset \mathbb{R}^n$ and $\mathbf{u}(t) \in \mathcal{U} \subset \mathbb{R}^m$, $n \geq m$, are the state and control vectors, respectively, \mathbf{f} is a smooth vector field, and $t \in \mathbb{R}$ is time. The system is *differentially flat* if the following definition holds.

Definition 1 (Adapted from [Rigatos \(2015\)](#)). A system described by (1) is said to be differentially flat if there exists a vector of *outputs* $\mathbf{y}(t) = (y_1(t), \dots, y_m(t))$, such that:

- (1) There exists a smooth function σ that maps $\mathbf{x}(t)$, $\mathbf{u}(t)$, and a finite number of its derivatives to \mathbf{y} , i.e.,

$$\mathbf{y}(t) = \sigma(\mathbf{x}(t), \mathbf{u}(t), \dot{\mathbf{u}}(t), \dots, \mathbf{u}^{(p)}(t)), \quad (2)$$

for some $p \in \mathbb{N}$.

- (2) The variables $\mathbf{x}(t)$ and $\mathbf{u}(t)$ can be expressed as smooth functions of $\mathbf{y}(t)$ and a finite number of its time derivatives, i.e.,

$$\mathbf{x}(t) = \gamma_0(\mathbf{y}(t), \dot{\mathbf{y}}(t), \dots, \mathbf{y}^{(q)}(t)), \quad (3)$$

$$\mathbf{u}(t) = \gamma_1(\mathbf{y}(t), \dot{\mathbf{y}}(t), \dots, \mathbf{y}^{(q)}(t)), \quad (4)$$

for some $q \in \mathbb{N}$.

- (3) The vectors $\mathbf{y}(t), i = 1, \dots, m$ and their time derivatives are differentially independent, i.e., there exists no differential relation satisfying $\eta(\mathbf{y}, \dot{\mathbf{y}}, \dots) = 0$.

Then the variables $y_i(t), i = 1, 2, \dots, m$ are the *outputs* of the differentially flat system.

Definition 1 implies a smooth bijective mappings σ, γ_0 , and γ_1 between the original space, $\mathcal{X} \times \mathcal{U}$, and a flat space \mathcal{Y} . Note that we employ dynamic extension to construct the flat space \mathcal{Y} using the output variables and a finite number of their derivatives. Furthermore, since this mapping uses only the original state variables and their derivatives, this is said to be an *endogenous* transformation. Next, we impose our working assumptions for the analysis of differentially flat systems that satisfy Definition 1.

Assumption 1. The trajectory of the system is contained in open set where the functions (2)–(4) exist.

Assumption 2. The control actions in the original and flat spaces are upper and lower bounded.

Assumption 1 is a standard assumption in the literature (see: [Van Nieuwstadt et al. \(1994\)](#)). It can be relaxed by constraining the trajectory to remain within a subset where (2)–(4) are defined, and several relaxations of this assumption are discussed in [Milam \(2003\)](#).

Assumption 2 is common in optimal control (see: [Bryson and Ho \(1975\)](#)), particularly for physical systems where actuators are ultimately bounded by their physical strength or energy consumption. This assumption can be relaxed by allowing the control input to take the form of a Dirac delta function, which introduces additional complexity that requires nonsmooth analysis.

Next, as an illustrative example of our approach, we introduce a “running” example that we will refer back to throughout the manuscript: a unicycle operating in \mathbb{R}^2 .

Example 1. Let $\mathbf{x}(t) = [p_x(t), p_y(t), \theta(t)]^T$ be the state of a unicycle in the \mathbb{R}^2 plane, where $p_x(t)$ and $p_y(t)$ denote the position, and $\theta(t)$ denotes the heading angle. Let $\mathbf{u}(t) = [u_1(t), u_2(t)]^T$ be the vector of control actions, where $u_1(t)$ and $u_2(t)$ denote the forward and angular velocity, respectively. Then, the dynamics are given by,

$$\dot{\mathbf{x}}(t) = \begin{bmatrix} u_1(t) \cos(\theta(t)) \\ u_1(t) \sin(\theta(t)) \\ u_2(t) \end{bmatrix}. \quad (5)$$

This system admits $m = 2$ differentially flat base states, $\mathbf{y}(t) = [y_1(t), y_2(t)]^T = [p_x(t), p_y(t)]^T$ (see: [Sira-Ramirez and Agrawal \(2018\)](#)). The transformations (3) and (4) between the flat and original variables are

$$\begin{bmatrix} p_x(t) \\ p_y(t) \\ \theta(t) \end{bmatrix} = \begin{bmatrix} y_1(t) \\ y_2(t) \\ \arctan2(\dot{y}_2, \dot{y}_1) \end{bmatrix}, \quad (6)$$

$$\begin{bmatrix} u_1(t) \\ u_2(t) \end{bmatrix} = \begin{bmatrix} \sqrt{\dot{y}_1(t)^2 + \dot{y}_2(t)^2} \\ \frac{\dot{y}_2 \dot{y}_1 - \dot{y}_2 \dot{y}_1}{\dot{y}_2^2 + \dot{y}_1^2} \end{bmatrix}, \quad (7)$$

which satisfy Assumption 1 for $u_1(t) \neq 0$.

Next, we formulate a constrained optimal control problem for a system governed by (1) under Assumptions 1 and 2.

Problem 1. Consider a differentially flat system (1) with running cost $L(\mathbf{x}(t), \mathbf{u}(t))$ over the time horizon

$[t^0, t^f] \subset \mathbb{R}$ and a final cost $\phi(\mathbf{x}(t^f), \mathbf{u}(t^f))$. Determine the optimal control input that minimizes the total cost, i.e.,

$$\begin{aligned} & \min_{\mathbf{u}(t)} \phi(\mathbf{x}(t^f), \mathbf{u}(t^f)) + \int_{t^0}^{t^f} L(\mathbf{x}(t), \mathbf{u}(t)) dt \\ & \text{subject to: (1),} \\ & \quad \hat{\mathbf{g}}(\mathbf{x}(t), \mathbf{u}(t), t) \leq 0, \\ & \text{given: initial conditions, final conditions,} \end{aligned}$$

where the initial and final states may be fixed, a function of the state variables, or left free. In addition, the function $\hat{\mathbf{g}}(\mathbf{x}(t), \mathbf{u}(t), t)$ defines a vector of state and control trajectory constraints.

In what follows, we present our main results, which yield a set of sufficient conditions for optimality that are only dependent on the state and control variables.

3 Main Results

3.1 Separability of the Optimality Conditions

First, we construct the flat space, which allows us to transform Problem 1 into an optimization over the differentially flat variables. Note that the transformations (3), (4), are a function of $\mathbf{y} = [y_1, y_2, \dots, y_m]$ and a finite number of their derivatives. Thus, we perform dynamic extension on each of our $i = 1, 2, \dots, m$ output variables y_i by taking k_i time derivatives. Note that the value of k_i is the minimum number of derivatives required to span the domain of (3) and (4), and thus it depends explicitly on the diffeomorphism in Definition 1. Using dynamic extension, we define analogous state and control variables for the system in the flat space.

Definition 2. Group each output y_i , $i = 1, \dots, m$ and their k_i derivatives into the state vector $\mathbf{s}(t)$ and control vector $\mathbf{a}(t)$ such that,

$$\mathbf{s}(t) = [y_1(t), \dots, y_1^{(k_1-1)}(t), \dots, y_m^{(k_m-1)}(t)]^T, \quad (8)$$

$$\mathbf{a}(t) = [y_1^{(k_1)}(t), \dots, y_m^{(k_m)}(t)]^T, \quad (9)$$

and $\mathbf{s} \times \mathbf{a} \in \mathcal{Y}$ span the flat space.

Remark 1. For the unicycle system in Example 1, the flat state and control variables are

$$\mathbf{s}(t) = [y_1(t), y_2(t), \dot{y}_1(t), \dot{y}_2(t)]^T, \quad (10)$$

$$\mathbf{a}(t) = [\ddot{y}_1(t), \ddot{y}_2(t)]^T, \quad (11)$$

which consists of two integrator chains, each with a length of $k_i = 2$, for $i = 1, 2$.

With the flat space completely defined, we apply the mappings (Definition 1) to construct an equivalent optimal control problem over the flat variables.

Problem 2. Find the cost-minimizing trajectory in the flat space,

$$\begin{aligned} & \min_{\mathbf{a}(t)} \Phi(\mathbf{s}(t^f), \mathbf{a}(t^f)) + \int_{t^0}^{t^f} \Psi(\mathbf{s}(t), \mathbf{a}(t)) dt \\ & \text{subject to: } \dot{\mathbf{s}} = \mathbf{I}(\mathbf{s}(t), \mathbf{a}(t)), \\ & \quad \mathbf{g}(\mathbf{s}(t), \mathbf{a}(t), t) \leq 0, \\ & \text{given: initial conditions, final conditions,} \end{aligned}$$

where \mathbf{I} denotes integrator dynamics, Φ , Ψ , \mathbf{g} , and the boundary conditions are constructed by composing ϕ , L , $\hat{\mathbf{g}}$, and the original boundary conditions of Problem 1 with the inverse of (3) and (4).

Under the framework proposed by Bryson and Ho (1975), we write the constraint \mathbf{g} with explicit dependence on the control action $\mathbf{a}(t)$. This is not restrictive on our analysis, and we rigorously prove in Section 3.3 that, under Assumption 2, any trajectory constraint $\mathbf{c}(\mathbf{s}(t), t)$ can be transformed into an explicit function of the control input. This is achieved by taking successive time derivatives of $\mathbf{c}(\mathbf{s}(t), t)$ until any component of the control vector $\mathbf{a}(t)$ appears; this yields a constraint with explicit functional dependence on the control variable and a set of tangency conditions that must be satisfied. This technique is similar to the derivation of control barrier functions with high relative degree, as discussed in Xiao and Belta (2019).

Note that solving Problem 2 yields the optimal solution to Problem 1 through Definition 1, and this construction is common in the literature (see Fliess et al. (1995); Petit et al. (2001); Milam (2003); Ogunbodede (2020) for examples). We present our first result next, which decouples the state and costates for the Hamiltonian function associated with Problem 2. Note that to simplify the notation, we omit the explicit dependence on $\mathbf{a}(t)$, $\mathbf{s}(t)$, and t for the remainder of this Section where it does not lead to ambiguity.

Theorem 1. The costates $\lambda^{y_i^{(j)}}$, for each base state $i = 1, 2, \dots, m$ and derivative $j = 0, 1, \dots, k_i - 1$, for Problem 2 are,

$$\lambda^{y_i^{(j)}} = \sum_{n=1}^{k_i-j} (-1)^n \frac{d^{n-1}}{dt^{n-1}} (\Psi_{y_i^{(j+n)}} + \boldsymbol{\mu}^T \mathbf{g}_{y_i^{(j+n)}}). \quad (12)$$

Proof. We follow the standard process of Bryson and Ho (1975); Ross (2015) for solving optimal control problems.

First, we construct the Hamiltonian for Problem 2,

$$\begin{aligned} H = \Psi(\mathbf{s}(t), \mathbf{a}(t)) + \boldsymbol{\lambda}^T(t) \mathbf{I}(\mathbf{s}(t), \mathbf{a}(t)) \\ + \boldsymbol{\mu}^T(t) \mathbf{g}(\mathbf{x}(t), \mathbf{a}(t), t), \end{aligned} \quad (13)$$

where $\boldsymbol{\lambda}(t)$ is the vector of costates, \mathbf{g} is a vector of inequality constraints, and $\boldsymbol{\mu}(t)$ is a vector of inequality Lagrange multipliers. The Euler-Lagrange and optimality equations are,

$$-\dot{\boldsymbol{\lambda}}^T = \Psi_{\mathbf{s}} + \boldsymbol{\lambda}^T \mathbf{I}_{\mathbf{s}} + \boldsymbol{\mu}^T \mathbf{g}_{\mathbf{s}}, \quad (14)$$

$$0 = \Psi_{\mathbf{a}} + \boldsymbol{\lambda}^T \mathbf{I}_{\mathbf{a}} + \boldsymbol{\mu}^T \mathbf{g}_{\mathbf{a}}, \quad (15)$$

where the subscripts \mathbf{a} and \mathbf{s} correspond to partial derivatives with respect to those variables. We simplify (14) by exploiting the integrator structure of \mathbf{I} for each element of $\mathbf{s}(t)$. This yields,

$$\dot{\lambda}^{y_i} = -\Psi_{y_i} - \boldsymbol{\mu}^T \mathbf{g}_{y_i}, \quad (16)$$

$$\dot{\lambda}^{y_i^{(j)}} = -\Psi_{y_i^{(j)}} - \lambda^{y_i^{(j-1)}} - \boldsymbol{\mu}^T \mathbf{g}_{y_i^{(j)}}, \quad (17)$$

for $i \in \{1, 2, \dots, m\}$ and $j \in \{1, 2, \dots, k_i - 1\}$. Similarly, simplifying each column of (15) yields

$$\lambda^{y_i^{(k_i-1)}} = -\Psi_{y_i^{(k_i)}} - \boldsymbol{\mu}^T \mathbf{g}_{y_i^{(k_i)}}, \quad (18)$$

for each base state $i \in \{1, 2, \dots, m\}$. Note that (18) satisfies (12) for $j = k_i - 1$. Next, taking a time derivative of (18) and substituting it into (17) with $j = k_i - 1$ yields

$$\frac{d}{dt} (\Psi_{y_i^{(k_i)}} + \boldsymbol{\mu}^T \mathbf{g}_{y_i^{(k_i)}}) = \Psi_{y_i^{(k_i-1)}} + \boldsymbol{\mu}^T \mathbf{g}_{y_i^{(k_i-1)}} + \lambda^{y_i^{(k_i-2)}},$$

which implies,

$$\begin{aligned} \lambda^{y_i^{(k_i-2)}} = & - \left(\Psi_{y_i^{(k_i-1)}} + \boldsymbol{\mu}^T \mathbf{g}_{y_i^{(k_i-1)}} \right) \\ & + \frac{d}{dt} \left(\Psi_{y_i^{(k_i)}} + \boldsymbol{\mu}^T \mathbf{g}_{y_i^{(k_i)}} \right), \end{aligned} \quad (19)$$

which satisfies (12) for $j = k_i - 2$. Taking repeated time derivatives of (19) and substituting (17) completes the proof of Theorem 1. \square

Theorem 1 could be interpreted as an alternative to the proof of separability presented in Chaplais and Petit (2008), however, our result is constructive and explicitly derives the costates as functions of state and control variables. Furthermore, our result relies on differential flatness, rather than feedback linearization, and does not require affinity with respect to the control inputs in the system dynamics. Furthermore, in the following subsections, we apply Theorem 1 to generate the optimal constrained trajectory and boundary conditions as a function of the state and control variable. This, to the best of our knowledge, has not been addressed to date.

Remark 2. For the unicycle system in Example 1, the covectors are,

$$\lambda^y = -(\psi_y + \mu^T g_y) + \frac{d}{dt}(\psi_a + \mu^T g_a), \quad (20)$$

$$\lambda^{y^{(1)}} = -(\psi_a + \mu^T g_a). \quad (21)$$

Our next result comes from manipulating Theorem 1 to eliminate the costate variables; this yields an equivalent optimality condition that is independent of the costate variables.

Theorem 2. The optimal trajectory for the system described in Problem 2 satisfies

$$\sum_{n=0}^{k_i} (-1)^n \frac{d^n}{dt^n} (\Psi_{y_i^{(n)}} + \mu^T g_{y_i^{(n)}}) = 0, \quad (22)$$

for each integrator chain starting with the base state y_i , $i = 1, 2, \dots, m$.

Proof. By Theorem 1,

$$\lambda^{y_i} = \sum_{n=1}^{k_i} (-1)^n \frac{d^{n-1}}{dt^{n-1}} (\Psi_{y_i^{(n)}} + \mu^T g_{y_i^{(n)}}). \quad (23)$$

Taking the derivative of (23) and substituting (16) yields,

$$\begin{aligned} \dot{\lambda}^{y_i} &= -\Psi_{y_i} - \mu^T g_{y_i} \\ &= \sum_{n=1}^{k_i} (-1)^n \frac{d^n}{dt^n} (\Psi_{y_i^{(n)}} + \mu^T g_{y_i^{(n)}}). \end{aligned} \quad (24)$$

This simplifies to

$$\Psi_{y_i} + \mu^T g_{y_i} + \sum_{n=1}^{k_i} (-1)^n \frac{d^n}{dt^n} (\Psi_{y_i^{(n)}} + \mu^T g_{y_i^{(n)}}) = 0, \quad (25)$$

which proves Theorem 2. \square

Note that while we prove Theorem 2 for the flat space, the mapping (3) and (4) can be composed with (22) to generate an equivalent optimality condition in the original space. Thus, the separation of states and costates is independent of the coordinate system, and is instead a fundamental property of differentially flat systems!

Remark 3. Applying Theorem 2 to Example 1 yields the optimality equation,

$$(\Psi_p + \mu^T g_p) - \frac{d}{dt}(\Psi_v + \mu^T g_v) + \frac{d^2}{dt^2}(\Psi_a + \mu^T g_a) = 0.$$

While Theorem 2 describes the evolution of the optimal state trajectory, one must also consider instantaneous jumps in the trajectory caused by constraints. Consider a constraint vector \mathbf{g} that has c linearly independent rows, then $\mu(t)$ is a $c \times 1$ matrix. When a constraint g_i , $i = 1, 2, \dots, c$ does not influence the system trajectory then $\mu_i(t) = 0$ by definition, otherwise $\mu_i(t) > 0$. When $\mu = \mathbf{0}$ the trajectory is said to follow a singular (unconstrained arc), and if any $\mu_i > 0$, then the trajectory is said to follow a regular (constrained) arc. When the system switches between singular and regular arcs, the corresponding costates may switch instantaneously at the so-called *constraint junction*.

We propose a new interpretation of this property, where the collection of singular and regular arcs constitute a set of *optimal motion primitives*. A vector of c constraints implies at most 2^c different motion primitives, which can be automatically computed using Theorem 2 and the corresponding constraint equations. In other words, Theorem 2 provides an *optimal motion primitive generator*, which can be solved numerically or analytically to derive every possible motion primitive.

In this context, dealing with switching elements of $\mu(t)$ is reduced to optimally switching between a finite set of motion primitives at unknown constraint junctions. The standard approach of Bryson and Ho (1975) derives optimality conditions that must be satisfied at each junction,

$$\lambda^{-T} = \lambda^{+T} + \pi^T \mathbf{N}_s, \quad (26)$$

$$H^+ - H^- = \pi^T \mathbf{N}_t, \quad (27)$$

$$\frac{\partial H^-}{\partial \mathbf{a}^-} = \frac{\partial H^+}{\partial \mathbf{a}^+} = \mathbf{0}, \quad (28)$$

where the superscripts $-$ and $+$ denote the instant in time just before and just after the the junction, respectively, π is a constant vector of Lagrange multipliers, \mathbf{N} is a vector of tangency conditions, which we rigorously derive in the following subsections, and the subscripts s and t correspond to partial derivatives with respect to the state and time. In the following subsections, we employ Theorem 1 to exhaustively write the jump conditions (26)–(28) as explicit functions of the state and control variables. This enables us to solve Problem 2 using only the state and control variables, which removes the numerical instabilities that are generally associated with nonlinear optimal control.

3.2 Interior-Point Constraints

First, we will consider the case where a set of state and/or control values are imposed at a single time instant. Let $\mathbf{h}(\mathbf{s}(t_1), t_1) = 0$ describe an interior point constraint that is imposed at some time t_1 . We construct

the tangency vector,

$$\mathbf{N}(\mathbf{s}(t), t) = \begin{bmatrix} \mathbf{h}(\mathbf{s}(t), t) \\ t - t_1 \end{bmatrix}, \quad (29)$$

which is necessary and sufficient for constraint satisfaction at t_1 when $\mathbf{N}(\mathbf{s}(t_1), t_1) = \mathbf{0}$. Note that if the time t_1 is unknown, then (29) reduces to $\mathbf{N} = \mathbf{h}$. To determine the optimal jump conditions, we substitute the tangency vector (29) into the optimality equations (26) and (27). Applying Theorem 1 to (26)–(28) yields $\sum_{i=1}^m \{k_i - 1\} + 1$ equations that determine the optimal change in \mathbf{a} and its derivatives at t_1 , and these equations are independent of the costate vectors.

Further manipulating (26)–(28) yields a useful pair of equations that are amenable to finding an analytical solution. First, we substitute (13) into (27) and use (26) to eliminate $\boldsymbol{\lambda}^-$,

$$\begin{aligned} (\Psi^+ - \Psi^-) + (\boldsymbol{\mu}^+ \mathbf{g}^+ - \boldsymbol{\mu}^- \mathbf{g}^-) \\ + \boldsymbol{\lambda}^{+T} (\mathbf{I}^+ - \mathbf{I}^-) = \boldsymbol{\pi}^T (\mathbf{N}_t + \mathbf{N}_s \mathbf{I}^-). \end{aligned} \quad (30)$$

Note that, by definition, $\boldsymbol{\mu}^T \mathbf{g} = 0$ along the optimal state-trajectory, thus we set those terms equal to zero. Furthermore, the state trajectory is continuous under Assumption 2 and the integrator dynamics. Thus,

$$\mathbf{I}^+ - \mathbf{I}^- = \begin{bmatrix} \mathbf{0} \\ \mathbf{a}^+ - \mathbf{a}^- \end{bmatrix}. \quad (31)$$

Applying Theorem 1 to (30) for the case $j = k_i - 1$ and simplifying yields,

$$\begin{aligned} (\Psi^+ - \Psi^-) - (\Psi_{\mathbf{a}} + \boldsymbol{\mu}^T \mathbf{g}_{\mathbf{a}})^- \cdot (\mathbf{a}^+ - \mathbf{a}^-) \\ = \boldsymbol{\pi}^T (\mathbf{N}_t + \mathbf{N}_s \mathbf{I}^+). \end{aligned} \quad (32)$$

Following a similar process also implies,

$$\begin{aligned} (\Psi^+ - \Psi^-) - (\Psi_{\mathbf{a}} + \boldsymbol{\mu}^T \mathbf{g}_{\mathbf{a}})^+ \cdot (\mathbf{a}^+ - \mathbf{a}^-) \\ = \boldsymbol{\pi}^T (\mathbf{N}_t + \mathbf{N}_s \mathbf{I}^-). \end{aligned} \quad (33)$$

3.3 Trajectory Constraints

Next, we consider the case when path constraints on the state and/or control variables are imposed on Problem 2 and influence the trajectory of the system. To generate our optimal motion primitive using Theorem 2, we first need to ensure our constraints are functions of the state and control variables. Let $h_i(\mathbf{s}(t), t) \leq 0$ denote the $i = 1, 2, \dots, c$ state or control constraints. Note that

h_i is not required to be an explicit function of the control input. Under the standard approach of Bryson and Ho (1975), we require that h_i is at least q_i -times differentiable, where q_i is the minimum number of derivatives required for any component of the control input to appear in $\frac{d^{q_i}}{dt^{q_i}} h_i$. To guarantee satisfaction of the original constraint h_i , we construct the tangency vector,

$$\mathbf{N}_i(\mathbf{s}(t), t) := \begin{bmatrix} h_i(\mathbf{s}(t), t) \\ h_i^{(1)}(\mathbf{s}(t), t) \\ \vdots \\ h_i^{(q_i-1)}(\mathbf{s}(t), t) \end{bmatrix}, \quad (34)$$

and define the constraint,

$$g_i(\mathbf{s}(t), \mathbf{a}(t), t) := h_i^{(q_i)}(\mathbf{s}(t), \mathbf{a}(t), t). \quad (35)$$

Thus, whenever $h_i(\mathbf{s}(t), t) = 0$ over a non-zero interval, we impose $\mathbf{N}_i(\mathbf{s}(t), t) = \mathbf{0}$ and $g_i(\mathbf{s}(t), \mathbf{a}(t)) = 0$ over the interior of the interval; this satisfies the original constraint under Assumption 2 (Bryson and Ho, 1975). Note that, if h_i is a function of the control variable, $q = 0$ and \mathbf{N}_i is empty. Furthermore, if the constraint is active over a zero-length interval, the problem reduces to the analysis in Section 3.2 with an unknown activation time.

Finally, to construct the tangency matrix for the c constraints, we construct the stacked tangency vector,

$$\mathbf{N}(\mathbf{s}(t), t) = \begin{bmatrix} \mathbf{N}_1(\mathbf{s}(t), t) \\ \mathbf{N}_2(\mathbf{s}(t), t) \\ \vdots \\ \mathbf{N}_c(\mathbf{s}(t), t) \end{bmatrix}, \quad (36)$$

which accounts for all of the constraints that may influence the state and control trajectory. As with the previous section, (26)–(28) determine the required instantaneous change in the control variables and their derivatives for an optimal trajectory.

Again, further manipulating (26)–(28) yields a pair of useful equations. Note that, by construction,

$$\boldsymbol{\pi}^T \dot{\mathbf{N}}^+ = 0, \quad (37)$$

as $\mathbf{N}_i = \mathbf{0}$ and $g_i^+ = 0$ when constraint i is active, and the corresponding $\boldsymbol{\pi}_i = 0$ otherwise. Thus, taking the full derivative implies

$$\boldsymbol{\pi}^T \dot{\mathbf{N}}^+ = \boldsymbol{\pi}^T (\mathbf{N}_t + \mathbf{N}_s \cdot \mathbf{I}^+) = \mathbf{0}. \quad (38)$$

Thus, applying (32) at the end of a constrained motion primitive yields

$$(\Psi^+ - \Psi^-) - (\Psi_{\mathbf{a}} + \boldsymbol{\mu}^T \mathbf{g}_{\mathbf{a}})^- \cdot (\mathbf{a}^+ - \mathbf{a}^-) = 0. \quad (39)$$

This leads directly to our next result,

Corollary 1. If the system exits from or enters to an unconstrained motion primitive, the optimal control input satisfies

$$\Psi^+ - \Psi^- - \Psi_{\mathbf{a}}^-(\mathbf{a}^+ - \mathbf{a}^-) = 0, \text{ or} \quad (40)$$

$$\Psi^+ - \Psi^- - \Psi_{\mathbf{a}}^+(\mathbf{a}^+ - \mathbf{a}^-) = 0, \text{ respectively.} \quad (41)$$

Proof. When the system exits from an unconstrained motion primitive, $\boldsymbol{\mu}^- = \mathbf{0}$ and the result follows by (39). When the system enters an unconstrained motion primitive, $\boldsymbol{\mu}^+ = \mathbf{0}$ and $\boldsymbol{\pi} = \mathbf{0}$, thus the result follows by (32). \square

Corollary 2. If the objective function has the form $\Psi = f(\mathbf{s}(t)) + \|\mathbf{a}(t)\|^2$, then the control input $\mathbf{a}(t)$ is always continuous when the system enters or exits an unconstrained motion primitive.

Proof. The proof follows trivially from Corollary 1 and continuity in $\mathbf{s}(t)$ from Assumption 2. \square

3.4 Boundary Conditions

The results of Sections 3.2 and 3.3 completely describe the evolution of the system if the boundary conditions are known. Next, we extend this result to the case that a boundary condition is unspecified by applying Theorem 1.

Corollary 3. Let the state $y_i^{(j)}(t)$ for $i \in \{1, 2, \dots, m\}$ and $j \in \{0, 1, 2, \dots, k_i - 1\}$ be unspecified at a boundary, i.e., it can be arbitrarily selected. There exists an equivalent boundary condition that guarantees optimality of the system trajectory.

Proof. Without loss of generality, let the state variable $y_i^{(j)}(t)$ be undefined at the final time t^f . Under the standard approach Bryson and Ho (1975), the corresponding boundary condition $\lambda y_i^{(j)}(t^f) = 0$ is required to guarantee optimality. Thus, by Theorem 1,

$$\sum_{n=1}^{k_i-j} (-1)^n \frac{d^{n-1}}{dt^{n-1}} (\Psi_{y_i^{(j+n)}} + \boldsymbol{\mu}^T \mathbf{g}_{y_i^{(j+n)}}) \Big|_{t^f} = 0 \quad (42)$$

is an equivalent boundary condition. \square

In practice, it is likely that Problem 2 will have boundary conditions defined by functions of the state variables. Without loss of generality, let $\mathbf{B}(\mathbf{s}(t^f), t^f) = \mathbf{0}$ describe the functional constraints at t^f . This implies that

$$\boldsymbol{\lambda}^T(t^f) = \left(\frac{\partial \Psi}{\partial \mathbf{s}} + \boldsymbol{\nu} \frac{\partial \mathbf{B}}{\partial \mathbf{s}} \right)_{t=t^f}, \quad (43)$$

$$\mathbf{B}(\mathbf{s}(t^f), t^f) = \mathbf{0}, \quad (44)$$

where $\boldsymbol{\nu}$ is a constant Lagrange multiplier that guarantees constraint satisfaction (see: Bryson and Ho (1975)). Applying Theorem 1 to (43) results in a system of equations that guarantees constraint satisfaction at the boundaries, which ensures that Problem 2 has the correct number of initial and final conditions.

Finally, it's possible that the boundary conditions are described at an unknown terminal time. In this case, the optimal terminal time t^f satisfies (Bryson and Ho, 1975)

$$\Omega = \left[\frac{\partial \Phi}{\partial t} + \boldsymbol{\nu} \frac{\partial \mathbf{B}}{\partial t} + \left(\frac{\partial \Phi}{\partial \mathbf{s}} + \boldsymbol{\nu}^T \frac{\partial \mathbf{B}}{\partial \mathbf{s}} \right) \mathbf{I} + \Psi \right]_{t=t^f} = 0. \quad (45)$$

Thus, Problem 2 always corresponds to a two-point boundary value problem with m initial conditions and m final conditions that are independent of the costates. Next, we present a numerical example for generating the trajectory of a double-integrator system in real time.

4 Crane Case Study

To demonstrate the effectiveness of our approach, we consider an overhead crane with a fixed rope length¹ as presented in Sun and Fang (2012); Chen et al. (2016); Zhang et al. (2017). Note that, to improve readability, we omit the explicit dependence of variables on time where it does not cause ambiguity. The overhead crane is modeled as a cart fixed to a rail, while the payload is modeled as a pendulum with negligible rope dynamics; this is illustrated in Fig. 1. Applying Newton's laws of motion to the crane system yields the dynamics,

$$\Sigma \begin{cases} (M + m)\ddot{p} + ml\ddot{\theta}\cos(\theta) - ml\dot{\theta}^2\sin(\theta) = F, \\ ml^2\ddot{\theta} + ml\cos(\theta)\ddot{p} + mgl\sin(\theta) = 0, \end{cases} \quad (46)$$

where M , m , l and g are parameters corresponding to the cart mass, payload mass, fixed rope length, and acceleration due to gravity, (p, θ) are the position of the cart and the payload swing angle, and the control variable F is a forward force applied to the cart. The first equation in (46) captures the linear dynamics of the cart, and the second equation couples the cart to the payload.

¹ Our code is available online at <https://github.com/Logiant/Flatness-Crane-Example>

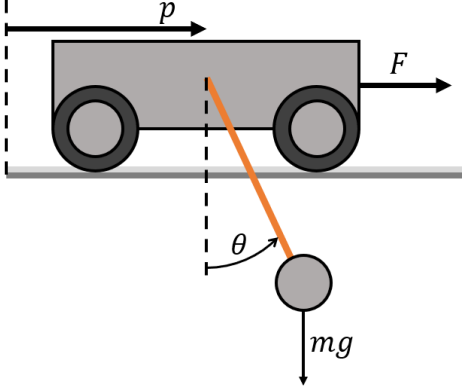


Fig. 1. The crane example; the cart at position p is driven along a fixed track by a force F . The load hangs at an angle θ by a rope of fixed length l .

The system (46) is differentially flat under the small angle approximation ($\sin(\theta) \approx \theta, \cos(\theta) \approx 1$), which is always satisfied for real applications [Chen et al. \(2016\)](#). Applying the small-angle approximation to the dynamics (46) and dividing the second equation by ml yields an approximation of the system,

$$\Sigma_a \begin{cases} (M+m)\ddot{p} + ml\ddot{\theta} - ml\dot{\theta}^2\theta = F \\ l\dot{\theta} + \ddot{p} + g\theta = 0. \end{cases} \quad (47)$$

The approximate system (47) is nonlinear and differentially flat with respect to the approximate payload position, $y = [p + l\theta]$. Taking two derivatives of y and substituting them into the second equation of (47) implies,

$$\theta = -\frac{\ddot{y}}{g}, \quad p = y + \frac{l}{g}\ddot{y}. \quad (48)$$

Taking successive derivatives of (48) and substituting them into (47) yields the control input F as a function of the flat variables,

$$F = (M+m)\left(\ddot{y} + \frac{l}{g}y^{(4)}\right) + ml\left(-\frac{y^{(4)}}{g} + \frac{\ddot{y}}{g}\left(\frac{y^{(3)}}{g}\right)^2\right), \quad (49)$$

and thus the approximate system is differentially flat with $k_i = 4$. Since 4 derivatives of the flat output y appear in (49), the state and action vectors for the optimization problem are,

$$\begin{aligned} \mathbf{s} &= [y, \dot{y}, \ddot{y}, y^{(3)}]^T, \\ \mathbf{a} &= y^{(4)}. \end{aligned} \quad (50)$$

To ensure no physical damage occurs during the transport process, we constrain the cart position p to remain

within predetermined bounds, i.e.,

$$p_{\min} \leq y + \frac{l}{g}\ddot{y} \leq p_{\max}. \quad (51)$$

The objective of the crane system is to deliver the hanging payload to a predetermined location with zero final velocity. We impose this through the boundary conditions, and we employ (48) and its derivatives to define the boundary conditions in the flat space,

$$\begin{bmatrix} y(t^0) \\ \dot{y}(t^0) \\ \ddot{y}(t^0) \\ y^{(4)}(t^0) \end{bmatrix} = \begin{bmatrix} p^0 + l\dot{\theta}^0 \\ \dot{p}^0 + l\dot{\theta}^0 \\ -g\theta^0 \\ -g\dot{\theta}^0 \end{bmatrix}, \quad \begin{bmatrix} y(t^f) \\ \dot{y}(t^f) \\ \ddot{y}(t^f) \\ y^{(4)}(t^f) \end{bmatrix} = \begin{bmatrix} p^f \\ 0 \\ 0 \\ 0 \end{bmatrix}. \quad (52)$$

Finally, during transit we seek to minimize the oscillation and jerk of the payload. We achieve this by minimizing the L^2 norm of the angular velocity $\dot{\theta}$, which also works to satisfy the small-angle assumption. We include a weighted jerk penalty as the L^2 norm of $y^{(4)}$, which also guarantees that Assumption 2 is satisfied and the optimal solution does not contain Dirac deltas (see [Bryson and Ho \(1975\)](#) for further details). The resulting optimal control problem is,

$$\min_{\mathbf{a}(t)} \frac{1}{2} \int_{t^0}^{t^f} \left(\frac{y^{(3)}}{g} \right)^2 + \left(\alpha y^{(4)} \right)^2 dt$$

subject to:

$$(52), \text{ integrator dynamics,}$$

$$p_{\min} \leq y + \frac{l}{g}\ddot{y} \leq p_{\max}.$$

Optimal Motion Primitives: We employ Theorem 2 to generate an ordinary differential equation that is sufficient for optimality,

$$\ddot{\mu} - \frac{y^{(6)}}{g^2} + \alpha^2 y^{(8)} - \frac{l}{g}\mu^{(4)} = 0. \quad (53)$$

This implies the form of the unconstrained optimal motion primitive,

$$\begin{aligned} y(t) &= c_0 + c_1 t + c_2 t^2 + c_3 t^3 + c_4 t^4 + c_5 t^5 \\ &+ c_6 \exp\left\{\frac{t}{\alpha g}\right\} + c_7 \exp\left\{\frac{-t}{\alpha g}\right\}, \end{aligned} \quad (54)$$

where c_0 - c_7 are constants of integration determined by the boundary conditions (52). Note that for problems with a fixed initial and terminal times, the constants of integration are the solution to an 8×8 system of linear equations that can be generated offline.

Next we derive the optimal constrained trajectory for the case that $p(t) = p_{\max}$; the same analysis holds for $p(t) = p_{\min}$. In this case, the trajectory satisfies,

$$y + \frac{l}{g}\ddot{y} = p_{\max}, \quad (55)$$

which has the general solution,

$$y(t) = c_8 \cos\left(\sqrt{\frac{g}{l}}t\right) + c_9 \sin\left(\sqrt{\frac{g}{l}}t\right) + p_{\max}, \quad (56)$$

where c_8, c_9 are constants of integration that are determined by the boundary conditions at the constraint junction. Note that (56) corresponds to the pendulum swinging freely while the constraint is active.

To avoid unnecessary complexity in this example, we introduce an additional assumption for this case study.

Assumption 3. The boundary conditions satisfy $p_{\min} < p^0, p^f < p_{\max}$, and the constraints bounding $p(t)$ are active over a non-zero interval of time.

We only employ Assumption 3 for brevity, and the switching behavior for an instantaneous constraint activation are straightforward to solve using the analysis in Section 3.2. For a case study that relaxes this assumption and only considers instantaneous constraint activation using our proposed approach, see [Beaver et al. \(2023b\)](#).

Switching Conditions: The unconstrained trajectory is a system of 8 equations and 8 unknowns, which are the boundary conditions (52) and trajectory coefficients (54) respectively. Under Assumption 3, if the unconstrained trajectory is infeasible then the system must transition to a constrained motion primitive for a finite interval of time. This introduces an additional 12 unknowns, 2 from the coefficients of the constrained motion primitive, 8 from the coefficients of the unconstrained motion primitive that follows, and 2 for the unknown junctions at the start and end of the constrained motion primitive. Following Section 3.3, we first construct the tangency conditions that must be satisfied when the systems enters the constrained motion primitive at time t_1 ,

$$N(\mathbf{s}(t_1)) = \begin{bmatrix} y(t_1) + \frac{l}{g}\ddot{y}(t_1) - p_{\max} \\ \dot{y}(t_1) + \frac{l}{g}y^{(3)}(t_1) \end{bmatrix} = \mathbf{0}. \quad (57)$$

We derive the corresponding 12 equations as follows:

- Assumption 2 yields 8 equations from continuity in $y, \dot{y}, \ddot{y}, y^{(3)}$ at the entry and exit of the constrained motion primitive.
- The tangency conditions (57) yield 2 equations at the entrance of the constrained motion primitive.

- Corollary 2 yields 2 equations from continuity in $y^{(4)}$ at the entry and exit of the constrained motion primitive.

Note that given a known sequence of transition times, each of the optimality conditions is linear with respect to the unknown constants of integration. Consider a solution with $k \geq 0$ segments. The initial and final conditions are captured by a set of linear equations,

$$A(t^0)\mathbf{c}_1 = \mathbf{b}_1, \quad (58)$$

$$A(t^f)\mathbf{c}_k = \mathbf{b}_k, \quad (59)$$

where A is a matrix that captures the structure of the unconstrained trajectory, \mathbf{c}_1 and \mathbf{c}_k contain the constants of integration for the initial and final unconstrained motion primitives, and $\mathbf{b}_1, \mathbf{b}_k$ are the initial and final conditions. If the system transitions to a constrained arc i at time t_i , this adds an additional system of equations,

$$\begin{aligned} A(t_i)\mathbf{c}_i &= \mathbf{z}_i, & (60) \\ \frac{c_6}{(\alpha g)^4} \exp\frac{t_i}{\alpha g} + \frac{c_7}{(\alpha g)^4} \exp\frac{-t_i}{\alpha g} + 24c_4 + 120c_5t_i \\ &= \frac{g^2}{l^2} \left(c_8 \cos\left(\sqrt{\frac{g}{l}}t_i\right) + c_9 \sin\left(\sqrt{\frac{g}{l}}t_i\right) \right), & (61) \end{aligned}$$

where the matrix A captures continuity in the state and the tangency conditions, \mathbf{c}_i is a vector of integration constants, \mathbf{z}_i captures continuity in the state variables and the tangency conditions, and (61) is continuity in $y^{(4)}$. Note that a similar structure holds when the system exits the constrained arc at some later time $t_{i+1} > t_i$.

Thus, to generate the optimal trajectory for a system with k segments, we need only to find the $k - 1$ zeros that correspond to solving (61) at each constraint junction. Given a potential solution t_k , we evaluate the linear system of equations (60) to generate the trajectory coefficients, and (61) determines whether the solution is optimal. Finally, we check the resulting solution to see if it is feasible. If it is not, then we introduce another constrained motion primitive and repeat the entire process.

Results: To demonstrate the performance of our approach, we simulated the crane system with the physical parameters listed in Table 1. We moved the crane from $p^0 = 0$ to $p^f = 5$ m over a period of $t^f - t^0 = 15$ s. As described in the problem statement, we set the initial speed and angular velocity to 0 along with the final speed, load angle, and angular speed. To ensure that the unconstrained trajectory overshoots past the limit of $p_{\max} = 10$, we we disturbed the load with an initial angle of $\theta^0 = -5$ deg.

We generated the optimal solution by solving (61) in Matlab2018b using the *fmincon* package; this is because the standard nonlinear solver is incapable of enforcing

M (kg)	m (kg)	g (m/s ²)	l (m)	α
200	50	9.81	5	0.5

Table 1
Parameters used for the crane simulation example

a monotonicity constraint on the junction times. On an i5-3570K (3.40 GHz), it took approximately 1.5 ms to generate the unconstrained optimal trajectory and 184 ms to generate the constrained solution.

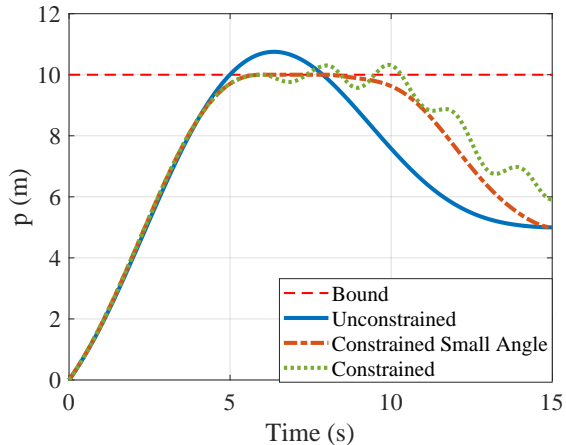


Fig. 2. Position of the cart following the unconstrained trajectory, constrained trajectory with the small-angle dynamics, and constrained trajectory with the original dynamics.

We performed three simulations, which are displayed in Figs. 2 and 3. In the first simulation we generated the unconstrained trajectory and simulated the crane’s motion with the full system dynamics (46). The resulting trajectory is smooth and continuous, but it violates the constraint that $p(t) \leq p_{\max}$. The second simulation is the optimal trajectory simulated using the small-angle approximation (47), which smoothly approaches the constraint boundary at $t = 6$ s and remains there until $t = 8$ s before smoothly transitioning to the final position $p = 5$ m. The final simulation simulates the original system dynamics (46) subject to the force F generated using (49). Note that in Fig. 3, while the constraint is active the angle of the load swings from $+12$ deg to -12 deg over 2 seconds. This significant angular velocity multiplies the the small-angle approximation, and causes the cart to oscillate around $p = p_{\max}$ while the constraint is active. Ultimately, due to this disturbance, the system is unable to reach the prescribed final state.

It is important to note that the inability of the original system to track our reference trajectory is a result of model mismatch between the original system and the differentially flat system. Furthermore, we applied our control in open-loop and did not employ a tracking controllers, e.g., control barrier functions, to track the desired trajectory. This is an open problem with the control of differentially flat systems, as any model error is amplified by the nonlinear diffeomorphism that map between

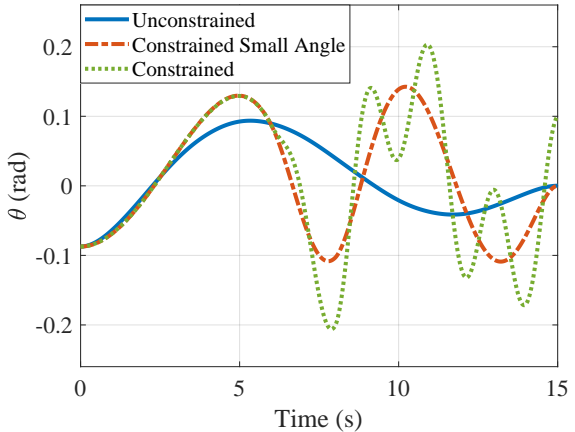


Fig. 3. Trajectory of the payload angle versus time for each of the simulations; there are significant oscillations in the constrained case, which use the original system dynamics.

the original and flat spaces. While there is some ongoing work to learn the minimize the model mismatch with learning techniques, e.g., Greeff and Schoellig (2021); Beaver et al. (2023a), an alternative approach may be to derive the optimal motion primitives in the original state space to avoid the issue of mismatch amplification.

5 Conclusion

In this paper, we proposed a technique to easily generate optimal trajectories for differentially flat systems. First, we derived an explicit ordinary differential equation that describes the optimal state evolution independently of the costates. Second, we applied the result of Theorem 1 to derive additional boundary conditions for the flat system, which has not been presented in the literature to the best of our knowledge. Third, we proposed a motion primitive generator in Theorem 2 and derived the conditions to optimally switch between different motion primitives. Finally, we applied our results in an illustrative case study, to generate a swing-minimizing trajectory for a nonlinear overhead crane system. We were able to generate trajectories on the order of milliseconds, and guarantee satisfaction of the boundary conditions while minimizing payload oscillation. Furthermore, this illustrative example is a concrete implementation of the theoretical contributions of this article.

There are several intriguing directions for future work. First, it is practical, for given dynamics, to determine what objective functions guarantee that an analytical solution to (22) exists. Another potential direction for future research is to relax Assumptions 1 and 2 and derive similar results for systems with singularities and unbounded actuation capabilities. Exploring problems with a large number of constraints, such as motion planning in cluttered environments, is another practical direction. Finally, developing a general-purpose numerical

method to formulate and solve optimization problems for differentially flat systems would be a valuable contribution.

Acknowledgements

The authors would like to thank Chris Kroninger and Michael Dorothy at DEVCOM Army Research Laboratory for their insightful technical discussions.

References

- L. E. Beaver and A. A. Malikopoulos. An Overview on Optimal Flocking. *Annual Reviews in Control*, 51:88–99, 2021.
- L. E. Beaver, B. Chalaki, A. M. Mahbub, L. Zhao, R. Zayas, and A. A. Malikopoulos. Demonstration of a Time-Efficient Mobility System Using a Scaled Smart City. *Vehicle System Dynamics*, 58(5):787–804, 2020.
- L. E. Beaver, M. Sokolich, S. Alsalehi, R. Weiss, S. Das, and C. Belta. Learning for control of rolling μ bots. *arXiv: 2212.00188*, 2023a.
- L. E. Beaver, R. Tron, and C. G. Cassandras. A graph-based approach to generate energy-optimal robot trajectories in polygonal environments. *arXiv: 2211.05251*, 2023b.
- A. E. Bryson, Jr. Optimal Control-1950 to 1985. *IEEE Control Systems Magazine*, 16(3):26–33, 1996.
- A. E. Bryson, Jr. and Y.-C. Ho. *Applied Optimal Control: Optimization, Estimation, and Control*. John Wiley and Sons, 1975.
- B. Chalaki, L. E. Beaver, A. M. I. Mahbub, H. Bang, and A. A. Malikopoulos. A research and educational robotic testbed for real-time control of emerging mobility systems: From theory to scaled experiments. *IEEE Control Systems*, 42(6):20–34, 2022.
- F. Chaplais and N. Petit. Inversion in indirect optimal control: constrained and unconstrained cases. In *46th IEEE Conference on Decision and Control*, pages 683–689, 2007.
- F. Chaplais and N. Petit. Inversion in indirect optimal control of multivariable systems. *ESAIM: COCV*, 14: 294–317, 2008.
- H. Chen, Y. Fang, and N. Sun. Optimal trajectory planning and tracking control methods for overhead cranes. *IET Control Theory & Applications*, 10(6): 692–699, 2016.
- M. Fliess, J. Levine, P. Martin, and P. Rouchon. Flatness and defect of non-linear systems: Introductory theory and examples. *International Journal of Control*, 61(6):1327–1361, 1995.
- K. Graichen, A. Kugi, N. Petit, and F. Chaplais. Handling constraints in optimal control with saturation functions and system extension. *Systems and Control Letters*, 59(11):671–679, 11 2010.
- M. Greeff and A. P. Schoellig. Exploiting Differential Flatness for Robust Learning-Based Tracking Control using Gaussian Processes. *IEEE Control System Letters*, 5(4):1121–1126, 2021.
- K. Jang, E. Vinitzky, B. Chalaki, B. Remer, L. Beaver, A. A. Malikopoulos, and A. Bayen. Simulation to scaled city: zero-shot policy transfer for traffic control via autonomous vehicles. In *Proceedings of the 10th ACM/IEEE International Conference on Cyber-Physical Systems*, pages 291–300, 2019.
- B. Kolar, H. Rams, and K. Schlacher. Time-optimal flatness based control of a gantry crane. *Control Engineering Practice*, 60:18–27, 3 2017.
- J. Lévine. On The Equivalence Between Differential Flatness and Dynamic Feedback Linearizability. *IFAC Proceedings Volumes*, 40(20):338–343, 2007.
- W. Li, S.-N. Chow, M. Egerstedt, J. Lu, and H. Zhou. Method of evolving junctions: A new approach to optimal path-planning in 2D environments with moving obstacles. *The International Journal of Robotics Research*, 36(4):403–413, 2017.
- A. M. I. Mahbub and A. A. Malikopoulos. Concurrent optimization of vehicle dynamics and power-train operation using connectivity and automation. In *SAE Technical Paper 2020-01-0580*. SAE International, 2020. doi: 10.4271/2020-01-0580.
- A. A. Malikopoulos, L. E. Beaver, and I. V. Chremos. Optimal time trajectory and coordination for connected and automated vehicles. *Automatica*, 125 (109469), 2021.
- D. Mellinger and V. Kumar. Minimum snap trajectory generation and control for quadrotors. In *IEEE International Conference on Robotics and Automation*, pages 2520–2525, 2011.
- M. B. Milam. *Real-Time Optimal Trajectory Generation for Constrained Dynamical Systems*. PhD thesis, California Institute of Technology, 2003.
- O. T. Ogunbodede. *Optimal Control of Differentially Flat Systems*. PhD thesis, The University at Buffalo, 2020.
- H. Oh, A. R. Shirazi, C. Sun, and Y. Jin. Bio-inspired self-organising multi-robot pattern formation: A review. *Robotics and Autonomous Systems*, 91:83–100, 2017.
- N. Petit, M. B. Milam, and R. M. Murray. Inversion Based Constrained Trajectory Optimization. *IFAC Proceedings Volumes*, 34(6):1211–1216, 2001.
- G. G. Rigatos. Differential flatness theory and flatness-based control. In *Studies in Systems, Decision and Control*, volume 25, pages 47–101. Springer International Publishing, 2015.
- I. M. Ross. *A Primer on Pontryagin’s Principle in Optimal Control*. Collegiate Publishers, San Francisco, 2nd edition, 2015.
- M. Rubenstein, C. Ahler, and R. Nagpal. Kilobot: A low cost scalable robot system for collective behaviors. In *Proceedings of the 2012 IEEE International Conference on Robotics and Automation*, pages 3293–3298, 2012.
- H. Sira-Ramirez and S. K. Agrawal. *Differentially Flat Systems*. CRC Press, 1st edition, 2018.

- K. Sreenath, N. Michael, and V. Kumar. Trajectory generation and control of a quadrotor with a cable-suspended load - A differentially-flat hybrid system. In *IEEE International Conference on Robotics and Automation*, pages 4888–4895, 2013.
- N. Sun and Y. Fang. New energy analytical results for the regulation of underactuated overhead cranes: An end-effector motion-based approach. *IEEE Transactions on Industrial Electronics*, 59(12):4723–4734, 2012.
- M. Van Nieuwstadt, M. Rathinam, and R. M. Murray. Differential flatness and absolute equivalence. In *Proceedings of the IEEE Conference on Decision and Control*, volume 1, pages 326–332, 1994.
- G. Vásárhelyi, C. Virágh, G. Somorjai, T. Nepusz, A. E. Eiben, and T. Vicsek. Optimized flocking of autonomous drones in confined environments. *Science Robotics*, 3(20), 2018.
- W. Xiao and C. Belta. Control Barrier Functions for Systems with High Relative Degree. In *Proceedings of the IEEE Conference on Decision and Control*, volume 2019-December, pages 474–479. Institute of Electrical and Electronics Engineers Inc., 12 2019.
- H. Zhai, M. Hou, F. Zhang, and H. Zhou. Method of evolving junction on optimal path planning in flows fields. *Autonomous Robots*, 46(8):929–947, 12 2022.
- Z. Zhang, Y. Wu, and J. Huang. Differential-flatness-based finite-time anti-swing control of underactuated crane systems. *Nonlinear Dyn*, 87:1749–1761, 2017.



Andreas A. Malikopoulos received the Diploma in mechanical engineering from the National Technical University of Athens, Greece, in 2000. He received M.S. and Ph.D. degrees from the department of mechanical engineering at the University of Michigan, Ann Arbor, Michigan, USA, in 2004 and 2008, respectively. He is the Terri Connor Kelly and John Kelly Career Development

Associate Professor in the Department of Mechanical Engineering at the University of Delaware, the Director of the Information and Decision Science (IDS) Laboratory, and the Director of the Sociotechnical Systems Center. Prior to these appointments, he was the Deputy Director and the Lead of the Sustainable Mobility Theme of the Urban Dynamics Institute at Oak Ridge National Laboratory, and a Senior Researcher with General Motors Global Research & Development. His research spans several fields, including analysis, optimization, and control of cyber-physical systems; decentralized systems; stochastic scheduling and resource allocation problems; and learning in complex systems. The emphasis is on applications related to smart cities, emerging mobility systems, and sociotechnical systems. He has been an Associate Editor of the *IEEE Transactions on Intelligent Vehicles* and *IEEE Transactions on Intelligent Transportation Systems* from 2017 through 2020. He is currently an Associate Editor of *Automatica*

and *IEEE Transactions on Automatic Control*. He is a member of SIAM, AAAS. He is also a Senior Member of IEEE, and a Fellow of the ASME.



Logan Beaver received the B.S. degree in mechanical engineering from the Milwaukee School of Engineering, Milwaukee, WI, USA, in 2015, the M.S. degree in mechanical engineering from Marquette University, Milwaukee, WI, USA, in 2017, and the Ph.D. degree in mechanical engineering from the University of Delaware, Newark, DE, USA in 2022. He is currently a postdoctoral associate in the Division of Systems Engineering at Boston University, Boston, MA, USA. His research interests are at the interface of complex systems, decentralized control, and optimization; his focus is on engineering decentralized robotic systems that take advantage of the mechanism of emergence. He is a member of the IEEE, SIAM ASME, and AAAS.